Infrared Photodissociation Spectroscopy of $Na(NH_3)_n$ Clusters: Probing the Solvent Coordination

Tom E. Salter, Victor Mikhailov,‡ and Andrew M. Ellis*

Department of Chemistry, University of Leicester, University Road, Leicester, LE1 7RH, United Kingdom

Received: May 12, 2007; In Final Form: June 22, 2007

The first mass-selective vibrational spectra have been recorded for $Na(NH_3)_n$ clusters. Infrared spectra have been obtained for $n = 3-8$ in the N−H stretching region. The spectroscopic work has been supported by ab initio calculations carried out at both the DFT(B3LYP) and MP2 levels, using a 6-311++G(d,p) basis set. The calculations reveal that the lowest energy isomer for $n \leq 6$ consists of a single solvation shell for the NH_3 molecules, although in the case of $n = 5$ and 6 there are two-shell isomers that are reasonably close in energy to the single-shell global potential energy minimum. The infrared spectra concur with the ab initio predictions, showing similar spectra for the $n = 3-6$ clusters but a marked change for $n = 7$ and 8. The change in spectroscopic features for $n \geq 7$ is indicative of molecules entering a second solvation shell, i.e., the inner solvation shell around the sodium atom can accommodate a maximum of six NH_3 molecules.

1. Introduction

Clusters of alkali metal atoms and solvent molecules have attracted considerable attention in recent years. One of the most fascinating and celebrated aspects of the solvation of alkali metals is the formation of solvated electrons.[1,2] These can form quite readily with the alkali metals because of the relatively low energy required to detach the valence electron. The most well-known case arises in the solvation of alkali metal atoms in ammonia, where transitions involving these electrons are responsible for the strong colors of the resulting solutions. Solvated electrons are also expected to form in finite clusters but the transition toward true solvated electron behavior as the cluster size grows is poorly understood.

The earliest experimental studies of alkali−ammonia clusters in the gas phase employed photoionization mass spectrometry.[3−7] The ionization thresholds deduced from these studies provided some interesting and tantalizing findings. In the case of $Na(NH_3)_n$, Hertel and co-workers found that the first adiabatic ionization energy falls rapidly from the alkali metal atom value as the solvent number, *n*, increases.[3] After $n = 4$ the ionization energy continues to fall but somewhat more slowly, eventually extrapolating to the bulk work function of liquid ammonia. One possible interpretation of these data is that the first solvation shell contains only four ammonia molecules, but the same research group has suggested that the shapes of the photoionization efficiency curves are more suggestive of a first solvation shell that can contain up to six ammonia molecules.[4] Clearly the photoionization data by themselves do not provide definitive structural information for $Na(NH_3)_n$ clusters.

To date ab initio calculations reported for $Na(NH_3)_n$ clusters have been restricted to a relatively low level of theory. Utilizing Hartree−Fock methodology with a 6-31+G(d) basis set, Hashimoto et al. have attempted to determine the key isomers for up to $n = 6$.[8,9] Although the calculated ionization energy trends as a function of cluster size matched those observed in the photoionization studies of Hertel and co-workers, the calculations were not definitive in establishing the size of the first solvation shell. Hashimoto et al. concluded that the first solvation shell was most likely complete for $n = 4$ or 5.

Previous spectroscopic studies of $Na(NH_3)_n$ have focused on the smallest clusters. $NaNH_3$ has been investigated by using matrix isolation infrared spectroscopy,[10] resonance-enhanced multiphoton ionization (REMPI) spectroscopy,[11,12] and ZEKE spectroscopy.[13] The REMPI technique is only suitable for the $n = 1$ cluster because in larger clusters the first excited electronic state is subject to rapid predissociation.[14] To avoid this problem, Brockhaus et al. have instead used mass-selective photodepletion spectroscopy in the visible and near-infrared regions to record size-selective electronic spectra of $Na(NH_3)_n$ clusters.[15] For $n \geq 3$ the spectral features begin to converge and show an absorption feature that is attributable to the lowest energy transition of a solvated electron. Little information on the structures of the clusters could be deduced from these spectra, although it was tentatively suggested that the widths of the bands and dependence of the band positions on *n* suggest a possible closing of the first solvation shell for $n = 4$.

The only other spectroscopic data extracted for sodium−ammonia clusters is from an infrared photodissociation study of $Na^+(NH_3)_n$ cations by Selegue and Lisy.[16] By using a tunable CO_2 laser to excite the umbrella vibration of the ammonia molecules, mass-selective infrared spectra were obtained. The absence of any vibrational predissociation of clusters for $n < 6$ was interpreted in terms of a closed first solvation shell at $n = 6$ in the cationic species.

The summary above shows that the size of the inner solvation shells in alkali−ammonia clusters is still a matter of debate. We have recently contributed to this topic by presenting the first mass-selective infrared spectra of $Li(NH_3)_n$ clusters.[17] The study of $Li(NH_3)_n$ clusters focused on the N−H stretching region and assignment of the spectra was achieved through comparison with ab initio calculations. Although the ab initio calculations were not able to reproduce all of the observed spectral features, they did successfully predict some of the main features seen in

* Address correspondence to this author. E-mail: andrew.ellis@le.ac.uk. Phone: +44 (0)116-252-2138. Fax: +44 (0)116-252-3789.

‡ Present address: School of Physics, University of Birmingham, Edgbaston, Birmingham B15 2TT, United Kingdom.

10.1021/jp073637e CCC: $37.00
Published on Web 07/28/2007

the infrared spectra, including the magnitude of the red-shift of the N−H stretching bands relative to those of free ammonia. The conclusion drawn for $Li(NH_3)_n$ was that the first solvation shell fills at $n = 4$.

In this paper we turn our attention to $Na(NH_3)_n$ clusters. We report the first vibrational spectra of these clusters and, in combination with ab initio calculations, have used these to determine structural information. The spectra are found to be consistent with an inner solvation shell that can accommodate up to six ammonia molecules, with a clear change in spectral features at $n = 7$ that indicates population of a second solvation shell.

2. Experimental Section

Full details of the experimental procedure have been provided elsewhere.[17] Briefly, sodium−ammonia clusters were formed in a supersonic molecular beam by a standard laser ablation technique. This involves ablation of a static sodium target by using the gently focused second harmonic (532 nm) output of a small Nd:YAG laser. Clusters were formed by expanding pure ammonia gas (BOC, >99.93%) at a maximum pressure of 2 bar through a pulsed nozzle. The metal atoms produced by laser ablation were picked up by the ammonia gas and passed down a clustering tube (∼5 mm) to allow metal−solvent cluster formation prior to expansion into vacuum. A skimmer was used to produce a molecular beam and about 30 cm downstream of the nozzle the beam enters the source region of a linear time-of-flight mass spectrometer.

The molecular beam is intersected in this region by the UV output from a tunable pulsed dye laser to photoionize the clusters by single photon absorption. To record a spectrum, we use a photodepletion technique similar to that described by Brockhaus et al.,[15] except in our case a tunable mid-infrared (IR) radiation source is employed to yield a vibrational spectrum. To achieve this, the photoionization laser pulse is preceded by an IR radiation pulse generated through the combination of a tunable pulsed dye laser with a hydrogen-filled multipass Raman shifter cell.[17] The IR pulse is timed to fire ∼50 ns prior to the photoionization laser, but it is worth noting that experiments have also been carried out in which this delay was varied from ∼0 through to several hundred nanoseconds with no significant impact on the infrared spectra. Ions were detected by using a time-of-flight mass spectrometer (TOF-MS) and subsequently recorded with a digital storage oscilloscope/PC combination.

3. Computational Details

To aid in the assignment of experimental data, ab initio calculations were undertaken on $Na(NH_3)_n$ clusters for $n = 1-7$, using GAUSSIAN 03.[18] To locate possible isomers a trial-and-error approach was employed, which began with simple Hartree−Fock calculations using a minimal basis set (STO-3G) to locate candidate structures by geometry optimization. These potential energy minima were then refined by using a larger basis set (6-311++G(d,p)) coupled with DFT (B3LYP) and MP2 methodology. To ensure that the geometry optimization algorithm found a true potential energy minimum, all calculations were run with no symmetry constraints to permit the variation of all $3N - 6$ degrees of freedom. All structures were checked by calculation of harmonic vibrational frequencies to ensure that they were real minima. Some of the minima found in the low-level calculations were found to survive in the higher level calculations, but others turned out to be transition states or switched to other isomeric forms. The trial-and-error approach we have adopted here is unlikely to succeed in finding all possible potential energy minima, especially for the larger clusters considered in this work. However, our primary concern has been to locate all of the low-lying isomers that might be of importance in the spectroscopic work and extensive trial-and-error investigation of the likely candidates makes us confident that all the important species have been identified.

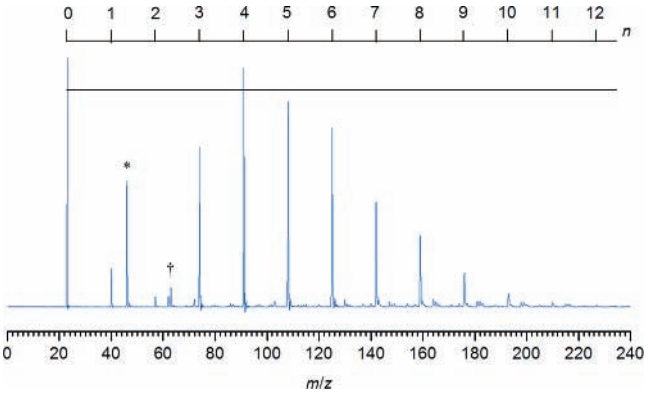

Figure 1. Mass spectrum obtained via photoionization at 387 nm. In addition to the series of peaks due to $Na(NH_3)_n^+$ clusters, there are also peaks due to Na_2^+ (*) and $Na_2NH_3^+$ (†).

For comparison with experiment, the calculated harmonic vibrational frequencies were scaled by 0.957 and 0.940 for DFT and MP2 calculations, respectively. These scaling factors were chosen to bring calculated N−H stretching vibrational frequencies of ammonia into best agreement with experiment.

4. Results

Figure 1 shows the mass spectrum obtained at a photoionization wavelength of 387 nm. At this wavelength only clusters with $n \geq 3$ are expected to be ionized by single photon ionization, explaining the small signal seen for the $n = 2$ ion. The substantial Na^+ and more modest $NaNH_3^+$ signals are the result of multiphoton ionization and most likely reflect the much higher abundance of the corresponding neutral species when compared to the larger $Na(NH_3)_n$ clusters.

Figure 2 shows infrared spectra recorded for $n = 3-8$ in the N−H stretching region. We have also attempted to record spectra for larger and smaller clusters, but outside of this selected range the signal-to-noise ratio was such that no clear structure could be discerned in the spectra. Consequently, all of our subsequent comments will focus on the $n = 3-8$ clusters. The baseline signal levels in the spectra in Figure 2 are somewhat uneven and reflect the difficulty in maintaining stable Na signals by laser ablation of a static target. To try and tackle this problem, some experiments were also attempted with a rotating/translating Na rod as the ablation target, but difficulties in achieving a sufficiently smooth surface for these rods led to no significant improvement over the static target approach. Consequently, in order to distinguish genuine spectral features from possible baseline fluctuations, several independent scans of the spectral region were recorded in each mass channel.

In addition to baseline fluctuations, there is also the issue of a cascade effect to consider in which photodepletion in one mass channel leads to ion photoproduction in another. Consider some cluster, $Na(NH_3)_n$, which undergoes IR-induced photodissociation to produce a smaller cluster, say $Na(NH_3)_{n-1}$. The photodissociation process will deplete the $Na(NH_3)_n^+$ signal but the production of an $Na(NH_3)_{n-1}$ fragment will, in isolation, increase the signal in the $Na(NH_3)_{n-1}^+$ channel. Competition between photodepletion and photoproduction could distort the IR spectrum and lead to misleading conclusions. In the case of previous

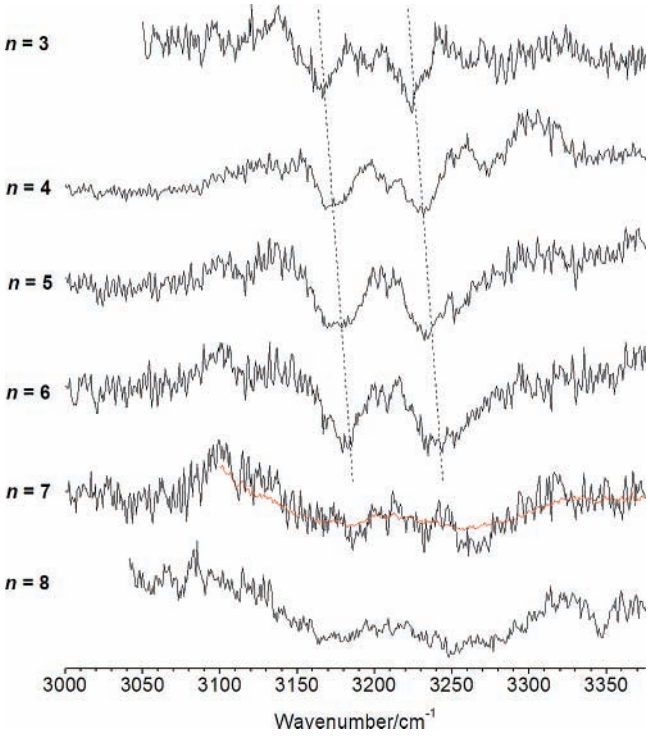

Figure 2. Infrared photodepletion spectra of $Na(NH_3)_n$ for $n = 3-8$. The $n = 4-8$ spectra were recorded simultaneously at a photoionization laser wavelength of 411 nm, while the $n = 3$ spectrum was recorded separately at a wavelength of 387 nm. The spectra were acquired with a step size of 0.7 cm^{-1} and 20 laser shots per wavelength. The smoother line in the $n = 7$ channel is the result of averaging 14 separate spectra, thus clarifying the broad absorption profile for this cluster.

work on $Li(NH_3)_n$ we were able to establish the dominance of ion photodepletion over photoproduction by showing that photodepletion bands observed in one channel show no matching photoproduction peaks in a lower mass channel.[17] Essentially the same argument can be applied here. For example, there is a weak, broad positive-going feature spanning 3100−3150 cm^{-1} in the $n = 4-7$ channels in Figure 2 that could conceivably be attributed to photoproduction from dissociation of larger clusters. However, if this is the case then a corresponding production signal in a higher mass channel would be expected, but there is no evidence of such a feature. On this basis we can rule out any significant contribution from photoproduction processes.

One factor that may serve to reduce photoproduction signals is the energy release on photodissociation, which can lead to some of the ion fragments moving out of the field of view of the microchannel plate detector during the journey through the time-of-flight mass spectrometer.[17] As discussed later, the dissociation energies of the $Na(NH_3)_n$ clusters are smaller than the corresponding $Li(NH_3)_n$ clusters, which may amplify this effect if a considerable proportion of the excess energy during photodissociation is released as fragment translational energy.

The infrared spectra for $n = 3-6$ consist of two bands between 3150 and 3250 cm^{-1}. These bands shift marginally to the blue as the cluster size increases, as indicated by the dashed lines in Figure 2, but otherwise show no significant changes as the cluster size increases. However, for $n = 7$ and 8 there is a marked change as the absorption features become much broader, so much so that it is now difficult to identify specific bands. The significance of these observations will be discussed below, taking each cluster in turn.

4.1. $Na(NH_3)_3$. The infrared spectrum of gaseous ammonia shows peaks in the N−H stretching region due to the N−H symmetric stretch (υ_1) at 3334 cm^{-1}, the N−H antisymmetric stretch (υ_3) at 3444 cm^{-1}, and the first overtone of the degenerate bending mode ($2\upsilon_4$) at 3217 ($l = 0$) and 3241 cm^{-1} ($l = 2$). The $2\upsilon_4$ overtone bands gain intensity through Fermi resonance with the fundamental modes.[19,20] The IR spectrum for $Na(NH_3)_3$ shows two depletion bands with maxima at 3165 and 3225 cm^{-1}. There is evidently a substantial red-shift for the N−H stretching bands in sodium−ammonia clusters when compared to free NH_3, an observation similar to that seen previously for $Li(NH_3)_n$ clusters and interpreted in terms of weakened N−H bonds due to the formation of metal−nitrogen bonds.[17] The alkali−nitrogen binding also has a dramatic effect on the intensity of the symmetric N−H stretching vibration relative to the antisymmetric N−H stretch. This was seen in our previous study of $Li(NH_3)_n$ and was also reported in the matrix isolation infrared investigation of $NaNH_3$ by Süzer and Andrews.[10]

Ab initio calculations carried out as part of this work predict that the lowest energy isomer of $Na(NH_3)_3$ has a trigonal arrangement of ammonia molecules about the central Na atom. This structure is in agreement with previous ab initio studies.[8,9] Comparison of the structures predicted by DFT and MP2 calculations reveals slight differences in the orientation of the ammonia molecules, but the trigonal arrangement is retained in both cases. A second isomer was found at higher energy, which was calculated to be 0.23 and 0.19 eV above the ground state isomer according to the DFT and MP2 calculations, respectively. In the higher energy isomer two NH_3 molecules are found in contact with the Na atom via Na−N bonds, while the third ammonia molecule is hydrogen bonded to one of the inner ammonia molecules. In this kind of structure we can describe those solvent molecules in intimate contact with the Na atom as being in the first solvation shell whereas the outer NH_3 is effectively in a second solvation shell. Accordingly, we label the ground state structure as a 3 + 0 isomer and the higher energy isomer as a 2 + 1 species, the first and second numbers referring to the number of solvent molecules in the first and second solvation shells, respectively. As a general rule, the lowest energy isomer maximizes contact of the NH_3 molecules with the Na atom because the Na−N bonding is much stronger than the hydrogen bonding between NH_3 molecules. Consequently, "surface" structures, where the Na atom is attached on the outside of a cluster of NH_3 molecules, are highly unfavorable energetically for alkali−ammonia clusters.

In Figure 3 the experimental $Na(NH_3)_3$ spectrum is compared to DFT simulations for the 3 + 0 and 2 + 1 isomers, where the simulated spectra have been created by fitting a convoluted Gaussian profile of fwhm = 10 cm^{-1} to the stick spectra. Simulated MP2 spectra show very similar results to DFT and so are not included here. The single peak in the simulation for the 3 + 0 isomer corresponds to a set of closely spaced transitions arising from excitation of the symmetric N−H stretch of the ammonia molecules, which reflects the high symmetry of the trigonal arrangement of solvent molecules. The red-shift of the symmetric N−H stretch relative to that of free ammonia seen in the experiment is approximately reproduced by the calculations, but the observation of at least two IR absorption bands is not.

The simulation for the 2 + 1 isomer shows an additional structure, which at first sight seems to accord more closely with the experimental spectrum. However, an assignment to the 2 + 1 isomer only is unlikely for several reasons. First of all, the 2 + 1 isomer is considerably higher in energy than the 3 + 0 isomer, and even if some of the 2 + 1 isomers were "frozen

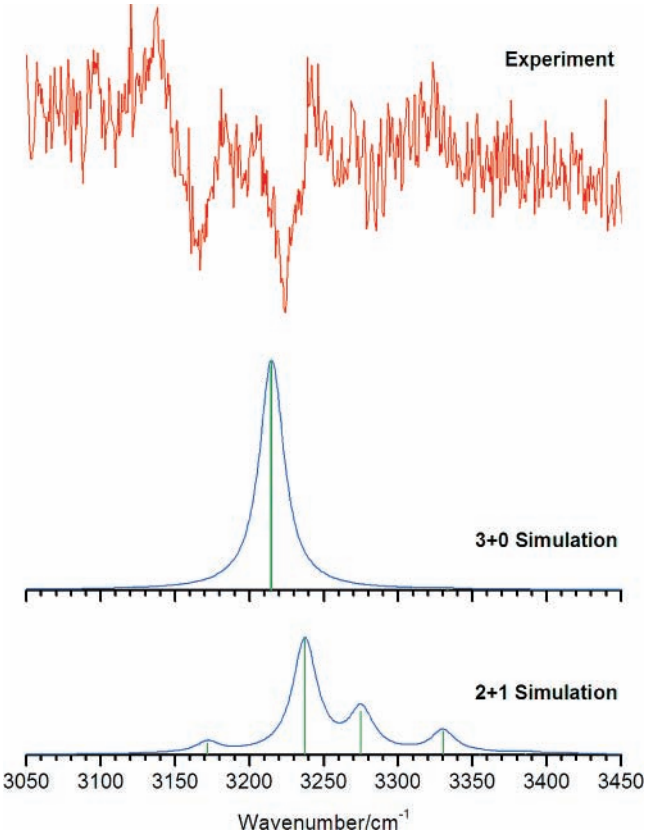

Figure 3. Experimental IR photodepletion spectrum of $Na(NH_3)_3$ (upper trace) and simulations derived from DFT calculations for the 3 + 0 isomer and the 2 + 1 isomer.

in" by rapid cooling in the supersonic expansion, the 3 + 0 isomer would still be expected to contribute substantially to the spectrum and would most likely dominate. Another argument against the 2 + 1 isomer is that the additional structure predicted by calculations does not match that observed in the experiment, either in terms of the number of bands nor their separations. Finally, we note that the harmonic vibrational calculations will be deficient in that they cannot account for anharmonic effects in the spectra. As mentioned above, the $2\upsilon_4$ overtone band is prominent in the infrared spectrum of gaseous ammonia due to Fermi resonance. This overtone may also be important in the infrared spectra of alkali−ammonia clusters and could be responsible for one of the bands in the spectrum shown in Figure 3.

The supporting ab initio calculations indicate that this is plausible. From the scaled vibrational frequencies we predict the $2\upsilon_4$ band to lie ~70 cm^{-1} below the N−H symmetric stretching band. Of course this is only a rough estimate, since no formal allowance is made for anharmonicity, for perturbation by Fermi resonance, and for the limitations of assuming a universal vibrational frequency scaling factor. Nevertheless, a band due to $2\upsilon_4$ is predicted on the low-frequency side of the symmetric N−H stretching band and in fact the separation between the two bands in the experimental spectrum of ~60 cm^{-1} is reasonably close to the ab initio estimate. We therefore tentatively assign the higher frequency band in the experimental spectrum in Figure 3 to the symmetric N−H stretching fundamental and the lower frequency band to the $2\upsilon_4$ overtone.

In the case of $Li(NH_3)_n$ clusters no IR-induced signal depletion was seen for $n < 4$. This was attributed to the higher dissociation energies possessed by the smaller clusters, which meant that absorption of a photon in the N−H stretching region was insufficient to bring about ejection of an ammonia molecule.

TABLE 1: Calculated Dissociation Energies (D_0 in cm^{-1}) for $Na(NH_3)_n$ Clusters

n	DFT	MP2	experiment[a]
1	2062	1763	3150 ± 200
2	2201	1766	2430 ± 200
3	2798	2400	2510 ± 200
4	2791	2561	3400 ± 200
5	1096	1285	2910 ± 200
6	1019	1195	2830 ± 200
7	730	679	

[a] The experimental values were obtained from conservation of energy arguments and employ the adiabatic ionization energy derived from photoionization threshold measurements[3] combined with experimental determinations of the dissociation energies of the corresponding cluster cations.[22]

We have used ab initio calculations to estimate the dissociation energies of $Na(NH_3)_n$ clusters and the results are shown in Table 1. The dissociation energies were calculated by using the supermolecule approach and the basis set superposition error was corrected by the counterpoise procedure. Only the lowest energy isomer for each cluster was considered. Also shown in Table 1 are dissociation energies from Nitsch and co-workers calculated using a combination of the cluster ionization energy (from photoionization threshold measurements[4]) and the dissociation energies of the cluster cations determined by Castleman and co-workers.[21]

The agreement between our calculated dissociation energies and those obtained by Nitsch and co-workers is, for most of the clusters, quite poor. In a previous study, we have attempted to calibrate the dissociation energies of clusters determined at the level of theory employed here with calculations carried out at higher levels of theory (CCSD(T) calculations with an aug-cc-pVQZ basis set).[22] This comparison leads us to expect that the most reliable calculated dissociation energies in the current work will come from the MP2 calculations and are unlikely to be in error by more than a few hundred wavenumbers. Consequently, the serious discrepancy between the "experimental" dissociation energies quoted in the third column of Table 1 and the ab initio values determined in the present work looks likely to originate from errors in the former quantities and presumably reflects either erroneous adiabatic ionization energies or inadequate cluster cation dissociation energies. At the present moment in time we do not know which of these possibilities is the source of the problem. What is clear from Table 1 is that excitation of N−H stretching fundamentals in all of the $Na(NH_3)_n$ clusters will deposit sufficient energy to remove an ammonia molecule. Consequently, the successful observation of a depletion spectrum for $Na(NH_3)_3$ but not for $Li(NH_3)_3$ is reasonable.

4.2. $Na(NH_3)_4$, $Na(NH_3)_5$, and $Na(NH_3)_6$. As mentioned earlier, the infrared spectra of $Na(NH_3)_4$, $Na(NH_3)_5$, and $Na(NH_3)_6$ bear a strong resemblance to that of $Na(NH_3)_3$. For $Na(NH_3)_4$, the ab initio calculations reveal a 4 + 0 structure as the lowest energy isomer, with an approximately tetrahedral arrangement of NH_3 molecules around the central Na atom. The next lowest energy isomer is a 3 + 1 cluster, whose energy separation from the 4 + 0 isomer is very similar to that calculated for the 3 + 0 and 2 + 1 isomers in $Na(NH_3)_3$. Ab initio simulation of the IR spectrum of the 3 + 1 isomer of $Na(NH_3)_4$ predicts a very different set of bands than for the 4 + 0 isomer. As with the 3 + 0/2 + 1 comparison for $Na(NH_3)_3$, the 3 + 1 isomer of $Na(NH_3)_4$ is predicted to yield a set of bands spread over a considerably wider spectral range than observed in the experimental spectrum. Consequently, since this

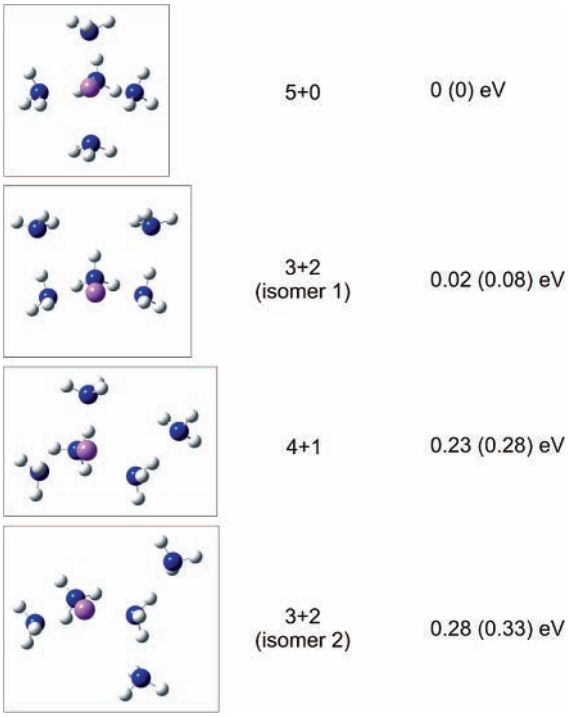

Figure 4. Predicted structures for $Na(NH_3)_5$. Relative energies from DFT and MP2 calculations are provided, with the MP2 values in parentheses

does not fit with the experimental spectrum, the dominant contributor is assigned to the 4 + 0 isomer.

The $n = 5$ and 6 isomers provide somewhat more of a challenge in terms of the ab initio calculations. Figures 4 and 5 show the lowest energy isomers calculated for these clusters. In both cases the lowest energy isomer is found to contain all of the solvent molecules in the inner solvation shell. However, in contrast to $Na(NH_3)_3$ and $Na(NH_3)_4$, the next lowest energy isomer is much closer in energy to the global minimum for $Na(NH_3)_5$ and $Na(NH_3)_6$. At the MP2 level, which is likely to predict this separation with greater accuracy than DFT, the separation is 0.08 eV for both $n = 5$ and 6. Figures 6 and 7 show the experimental IR spectra along with simulations for the two lowest energy isomers. If both isomers were to make substantial contributions to the experimental spectrum, then the simulations would lead us to expect the spectral profiles to change markedly when compared to those of the $n = 3$ and 4 clusters. According to the simulations this would be most profound for the $n = 5$ cluster, which should show additional bands to higher and lower wavenumbers than those seen for $n = 3$ and 4. Some contribution from the higher energy isomers cannot be ruled out, but the comparison between theory and experiment, coupled with the strong similarity of the band shapes and positions to those of the $n = 3$ and 4 clusters, favors the single-shell isomers as the dominant spectral carriers. The energy separation between isomers, although smaller for $n = 5$ and 6, still seems to be sufficient to maintain most of the population in the lowest energy isomer. Given the strong similarities for all of the $n = 3-6$ clusters, the infrared spectra support the notion that all of the ammonia molecules reside in the inner solvation shell and thus this inner shell can hold at least six ammonia molecules.

As with $Na(NH_3)_3$, we assume that the presence of a second, lower frequency band in the experimental spectra for $n = 4-6$ is due to excitation of the $2\upsilon_4$ overtone. On the basis of this assignment the ab initio calculations do an excellent job in predicting the absolute position of the N−H stretching fundamental. The calculations also successfully reproduce the progressive shift of the N−H stretching bands to the blue as n increases, as seen in the experimental spectra.

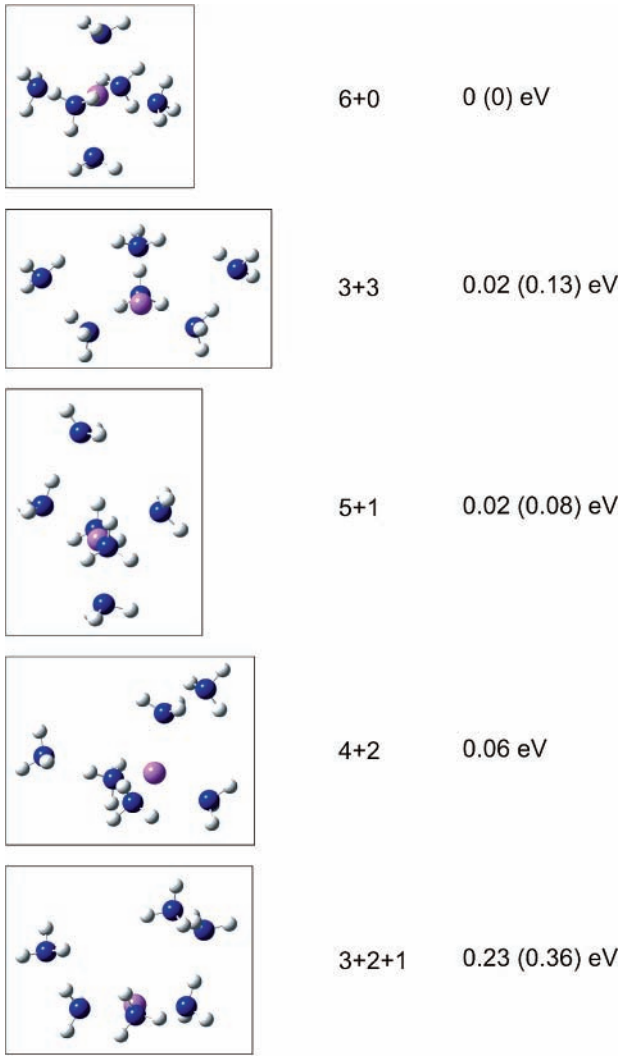

Figure 5. Predicted structures for $Na(NH_3)_6$. Relative energies from DFT and MP2 calculations are provided, with the MP2 values in parentheses. Note that for the 4 + 2 isomer only the DFT calculation successfully converged.

4.3. $Na(NH_3)_7$ and $Na(NH_3)_8$. The IR depletion spectrum of $Na(NH_3)_7$ has a different appearance from those observed for smaller sodium−ammonia clusters described above. The identification of structural features is more challenging owing to the poor signal-to-noise level, but what is evident is that the two distinct bands have been replaced by much broader absorption features extending over more than 200 cm^{-1}. This is most clearly seen in the highly averaged spectrum in Figure 2 superimposed on a much noisier single spectral scan.

To try and interpret this spectrum *ab initio* calculations were undertaken but these were not as extensive and definitive as in the case of the smaller clusters because of the associated computational expense. Consequently, only a limited number of starting configurations were employed, which were geared mainly to establishing whether or not all seven ammonia molecules could fit into the first solvation shell. Despite several attempts utilizing a variety of 7 + 0 starting geometries, optimization resulted either in no stationary point or in a structural change to yield a two-shell isomer. The global minimum for the $n = 7$ cluster was found to be a 6 + 1 species in which the inner solvation shell contains six ammonia

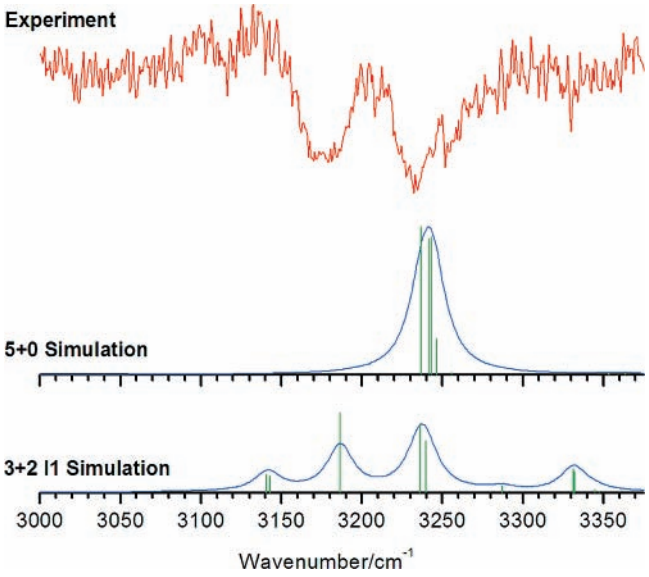

Figure 6. Experimental IR photodepletion spectrum of $Na(NH_3)_5$ (upper trace) above simulations for the 5 + 0 and the 3 + 2 (isomer 1) clusters.

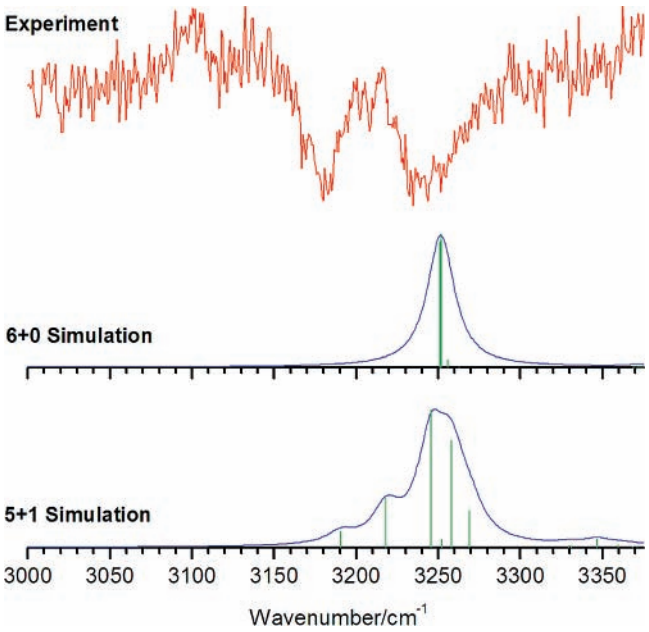

Figure 7. Experimental IR photodepletion spectrum of $Na(NH_3)_6$ (upper trace) above simulations for the 6 + 0 and 5 + 1 isomers.

molecules, roughly arranged in an octahedral geometry, and the seventh ammonia molecule is located in the second solvation shell via hydrogen bonds to two inner shell ammonia molecules. This structure was obtained independently by both DFT and MP2 calculations.

In Figure 8 the experimental spectrum is compared with a simulation from DFT calculations. The simulated spectrum consists of a number of transitions which produce a much broader composite peak than was the case for single shell isomers. These additional transitions are partly the result of the lower symmetry of the $n = 7$ cluster when compared with the global minima of the smaller clusters, coupled with band shifts due to the presence of an NH_3 molecule in a very different environment compared with the inner shell solvent molecules. The predicted broadening is consistent with the marked increase broadening seen in the experimental spectrum in moving from $n = 6$ to 7, and thus we can account for the observed IR spectrum of $Na(NH_3)_7$ by invoking solvent occupation of a

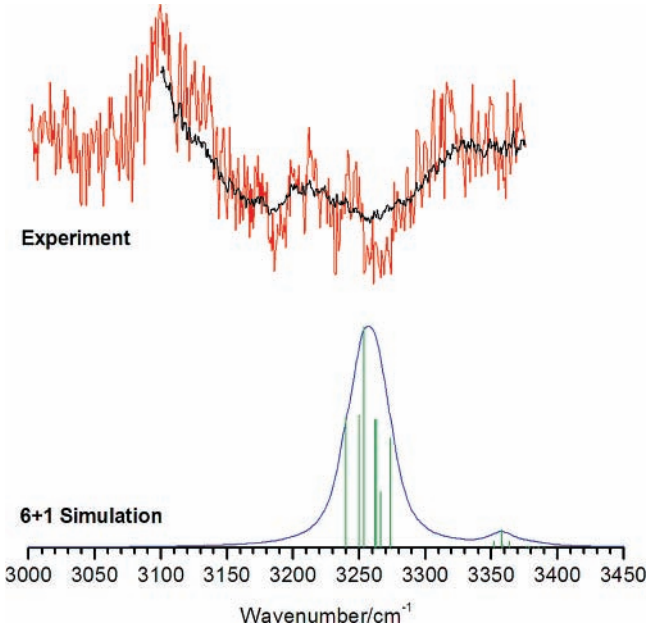

Figure 8. Experimental IR photodepletion spectrum of $Na(NH_3)_7$ (upper trace) above a simulation for the 6 + 1 isomer. The smoother black line through the experimental spectrum is an average of 14 separate scans of the $n = 7$ spectrum in order to confirm the band profiles.

second solvation shell. As with the smaller clusters, we expect contributions not only from the N−H stretching bands but also $2\upsilon_4$ overtone features, which again are likely to be broadened relative to the single-shell clusters.

Although the signal-to-noise ratio in the IR depletion spectrum of $Na(NH_3)_8$ in Figure 2 is poor, the same degree of spectral broadening observed for $Na(NH_3)_7$ seems to occur for $Na(NH_3)_8$. Due to the size of this cluster and the potential for a highly complex conformational landscape, no ab initio calculations were attempted for the $n = 8$ cluster. However, by analogy with $Na(NH_3)_7$ we propose that a two-shell structure, most likely a 6 + 2 isomer, is primarily responsible for the observed spectrum.

5. Discussion

Our interpretation of the IR spectra of the $Na(NH_3)_n$ clusters for $n = 3-8$ suggests that up to six ammonia molecules can fit into the first solvation shell, a conclusion supported by ab initio calculations. This contrasts sharply with $Li(NH_3)_n$, where both theory and experiment lead to the conclusion that only four NH_3 molecules can fit into the first solvation shell.[17] The difference between lithium and sodium solvation clearly arises from the difference in atomic radii. In the case of $Na(NH_3)_n$ clusters the equilibrium Na−N distances for the inner shell molecules are calculated to be in the region of 2.5 Å whereas the Li−N distances in $Li(NH_3)_n$ are <2.1 Å. Consequently, there is more room available in the case of $Na(NH_3)_n$ clusters to squeeze additional NH_3 molecules into the inner solvation shell.

It is interesting to compare the results from this gas-phase study with the findings from neutron diffraction studies of sodium−ammonia solutions.[23,24] The most recent investigation, carried out by Wasse and co-workers, obtained an average Na coordination number of ∼5.5 ammonia molecules.[24] In addition, the average Na−N distance in the first solvation shell was found to lie in the range 2.45−2.50 Å, which is very similar to the Na−N distances predicted by the ab initio calculations reported in the present work. The fact that an integer number of solvent molecules was not identified is explained by the calculations

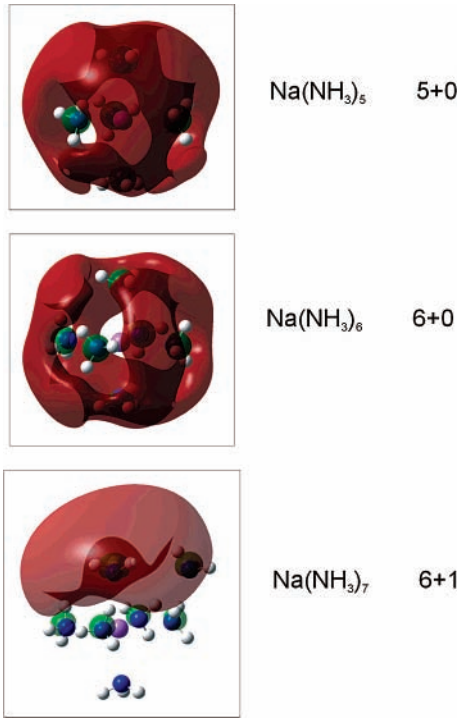

Figure 9. SOMO electron density contour plots obtained from MP2 calculations for the lowest energy isomers of $Na(NH_3)_5$, $Na(NH_3)_6$, and $Na(NH_3)_7$.

reported here, which suggest that single-shell and two-shell structures lie reasonably close together in energy for the $n = 5$ and 6 clusters. In the condensed phase it obviously invalid to think in terms of specific, isolated isomers, and the structural energetics will inevitably be altered by the presence of a bulk solvent. This may facilitate fluxional interchange between five- and six-coordinated structures and, in a practical sense, it may be inappropriate to think in terms of a rigid 6-fold coordination of Na in Na/NH_3 solutions. Nevertheless, it is pleasing to see that the conclusions drawn from the present gas-phase study do concur largely with the findings from structural studies of bulk sodium−ammonia solutions.

Finally, the impact of the closing of the solvation shell on the unpaired electron density distribution is considered because of its relevance to the solvated electron issue discussed in the Introduction. Hashimoto and Morokuma have previously generated electron density plots for the semioccupied molecular orbital (SOMO) in $Na(NH_3)_n$ clusters for up to $n = 6$ but, as mentioned earlier, their lower level calculations predicted a closing of the inner solvation shell at $n = 5$,[9] whereas we find that this shell can accommodate up to six ammonia molecules. In Figure 9 we show SOMO electron density contour plots obtained from MP2 calculations for the lowest energy isomers of $Na(NH_3)_5$, $Na(NH_3)_6$, and $Na(NH_3)_7$. For $Na(NH_3)_5$ the SOMO profile is similar to that reported by Hashimoto and Morokuma, showing a diffuse Rydberg-like orbital where the SOMO density is primarily located in the gaps between solvent molecules within the solvation shell. A similar scenario is found for $Na(NH_3)_6$, but for $Na(NH_3)_7$ there is a major change. With the addition of a single ammonia molecule into the second solvation shell the electron is no longer distributed around the sodium atom but instead fully detaches and moves to the outer surface of the inner solvation shell and beyond. Occupation of the second solvation shell clearly triggers a process that begins to resemble fully solvated electron behavior. It would be interesting to explore this further by carrying out ab initio calculations on larger clusters, but such calculations will be challenging because of the considerable computational resources required.

6. Conclusions

The first mass-selective vibrational spectra have been recorded for $Na(NH_3)_n$ in the N−H stretching region. The infrared spectra for the $n = 3-6$ clusters are remarkably similar and suggest a common structural arrangement of ammonia molecules about the Na atom. Ab initio calculations support this conclusion, finding that for $n = 3-6$ the global potential energy minimum contains all of the solvent molecules in the inner solvation shell. However, for $n = 7$ the global minimum is predicted to be a two-shell isomer consisting of six ammonia molecules in the first solvation shell and one additional molecule in the second solvation shell. This prediction concurs with the marked change in spectral features in moving from the $n = 6$ to 7 mass channel, which manifests itself as more extensive spectral broadening in the case of $n = 7$. Both the IR and ab initio data therefore provide evidence that the first solvation shell in sodium−ammonia clusters is able to accommodate up to six ammonia molecules.

Acknowledgment. The authors are grateful for financial support from the UK Engineering and Physical Sciences Research Council and from the Royal Society. The EPSRC National Service for Computational Chemistry is also gratefully acknowledged for providing both software and hardware resources in support of this work.

References and Notes

(1) Hart, E. J.; Anbar, M. *The hydrated electron*; Wiley: New York, 1970.

(2) Feng, D.-F.; Kevan, L. *Chem. Rev.* **1980**, *80*, 1.

(3) Hertel, I. V.; Hüglin, C.; Nitsch, C.; Schulz, C. P. *Phys. Rev. Lett.* **1991**, *67*, 1767.

(4) Nitsch, C.; Schulz, C. P.; Gerber, A.; Zimmermann-Edling, W.; Hertel, I. V. *Z. Phys. D* **1992**, *22*, 651.

(5) Takasu, R.; Hashimoto, K.; Fuke, K. *Chem. Phys. Lett*. **1996**, *258*, 94.

(6) Takasu, R; Misaizu, F.; Hashimoto, K.; Fuke, K. *J. Phys. Chem. A* **1997**, *101*, 3078.

(7) Stenbach, C.; Buck, U. *J. Chem. Phys.* **2005**, *122*, 134301.

(8) Hashimoto, K.; He, S.; Morokuma, K. *Chem. Phys. Lett.* **1993**, *206*, 297.

(9) Hashimoto, K.; He, S.; Morokuma, K. *J. Am. Chem. Soc.* **1995**, *117*, 4151.

(10) Süzer, S.; Andrews, L. *J. Am. Chem. Soc.* **1987**, *109*, 300.

(11) Nitsch, C.; Hüglin: Hertel, I. V.; Schulz, C. P. *J. Chem. Phys.* **1994**, *101*, 6569.

(12) Schulz, C. P.; Nitsch, C. *J. Chem. Phys.* **1997**, *107*, 9794.

(13) Rodham, D. A.; Blake, G. A. *Chem. Phys. Lett.* **1997**, *264*, 522.

(14) Schulz, C. P.; Höhndorf, J.; Brockhaus, P.; Noack, F.; Hertel, I. V. *Chem. Phys. Lett.* **1995**, *239*, 18.

(15) Brockhaus, P.; Hertel, I. V.; Schulz, C. P. *J. Chem. Phys.* **1999**, *110*, 393.

(16) Selegue, T. J.; Lisy, J. M. *J. Phys. Chem.* **1992**, *96*, 4143.

(17) Salter, T. E.; Mikhailov, V. A.; Evans, C. J.; Ellis, A. M. *J. Chem. Phys.* **2006**, *125*, 034302.

(18) Frisch, M. J.; Trucks G. W.; Schlegel, H. B.; Scuseria, G. E.; Robb, M. A.; Cheeseman, J. R.; Montgomery, J. A., Jr.; Vreven, T.; Kudin, K. N.; Burant, J. C.; Millam, J. M.; Iyengar, S. S.; Tomasi, K.; Barone, V.; Mennucci, B.; Cossi, M.; Scalmani, G.; Rega, N.; Petersson, G. A.; Nakatsuji, H.; Hada, M.; Ehara, M.; Toyota, K.; Fukuda, R.; Hasegawa, J.; Ishida, M.; Nakajima, T.; Honda, Y.; Kitao, O.; Nakai, H.; Klene, M.; Li, X.; Knox, J. E.; Hratchian, H. P.; Cross, J. B.; Bakken, V.; Adamo, C.; Jaramillo, J.; Gomperts, R.; Stratmann, R. E.; Yazyev, O.; Austin, A. J.; Cammi, R.; Pomelli, C.; Ochterski, J. W.; Ayala, P. Y.; Morokuma, K.; Voth, G. A.; Salvador, P.; Dannenberg, J. J.; Zakrzewski, V. G.; Dapprich, S.; Daniels, A. D.; Strain, M. C.; Farkas, O.; Malick, D. K.; Rabuck, A. D.; Raghavachari, K.; Foresman, J. B.; Ortiz, J. V.; Cui, Q.; Baboul, A.

G.; Clifford, S.; Cioslowski, J.; Stefanov, B. B.; Liu, G.; Liashenko, A.; Piskorz, P.; Komaromi, I.; Martin, R. L.; Fox, D. J.; Keith, T.; Al-Laham, M. A.; Peng, C. Y.; Nanayakkara, A.; Challacombe, M.; Gill, P. M. W.; Johnson, B.; Chen, W.; Wong, M. W.; Gonzalez, C.; Pople, J. A. *Gaussian 03*, Revision C.02; Gaussian, Inc.: Wallingford, CT, 2004.

(19) Beu, T. A.; Buck, A. *J. Chem. Phys.* **2001**, *114*, 7853.

(20) Guelachvili, G.; Abdullah, A. H.; Tu, N.; Narahari Rao, K.; Urban, A. A.; Papousek, D. *J. Mol. Spectrosc.* **1989**, *133*, 345.

(21) Castleman, A. W., Jr.; Holland, P. M.; Lindsay, D. M.; Peterson, K. I. *J. Am. Chem. Soc.* **1978**, *100*, 6039.

(22) Salter, T. E.; Ellis, A. M. *Chem. Phys.* **2007**, *332*, 132.

(23) Wasse, J. C.; Stebbings, S. L.; Masmanidis, S.; Hayama, S.; Skipper, N. T. *J. Mol. Liq.* **2002**, *96*−*7*, 341.

(24) Wasse, J. C.; Hayama, S.; Masmanidis, S.; Stebbings, S. L.; Skipper, N. T. *J. Chem. Phys.* **2003**, *118*, 7486.